NAIC-ID(RS)T-0150-96

NATIONAL AIR INTELLIGENCE CENTER

SELECTED ARTICLES

HUMAN TRANSLATION

NAIC-ID(RS)T-0150-96 1 October 1996

MICROFICHE NR:

SELECTED ARTICLES

English pages: 48

Source: Jiguang Jishu (Laser Technology), Vol. 13, Nr. 1, February 1989; pp. 14-20; 27-34; 46-50

Country of origin: China
Translated by: SCITRAN
F33657-84-D-0165
Requester: NAIC/TATD/Bruce Armstrong
Approved for public release: distribution unlimited.

TABLE OF CONTENTS

GRAPHICS DISCLAIMER

All figures, graphics, tables, equations, etc. merged into this translation were extracted from the best quality copy available.

LASER RECEIVING AND AIMING SYSTEM

Yu Jinxiang

Translation of "Ji Guang Jie Shou Yu Miao Zhun He Yi Guang Xue Xi Tong She Ji"; Laser Technology, Vol.13, No.1, pp 14-20

ABSTRACT

What this article discusses are optical systems. They are optical antennas developed for ship borne fire control laser range finders. The antennas in question have already been mounted and are in practical use. They possess the two functions of laser reception as well as observation and aiming. In the article, the operating principles and parameter determination of the combined optical systems in question are introduced. Discussion is made of dual wave band spectral methods associated with reception and aiming and the handling of image aberrations. Design results are given.

I. INTRODUCTION

As far as ship borne fire control laser range finders are concerned, they are installed on radar and television tracking fire control systems and used in range finding against maneuvering air and sea targets.

With respect to aerial fire control laser range finding devices associated with land artillery and ship guns, option is normally made for the use of optical antennas. These are composed of three independent transmission, reception, and aiming systems. In regard to the engineering prototype which we developed (it received a first level award for scientific and technical progress in the electronic section), it was also made up of three optical transmission, reception, and aiming systems. In order to reduce a step further the volume and weight of the apparatus as a whole, raising and improving overall performance,

increasing equipment flexibility, and expanding the range of utilizations--on the foundation of the engineering prototype--successful development was done of optical antennas combining laser reception, observation, and aiming in one, thus making performance of the whole apparatus, mounting precisions, overall lay out, volume, weight, and flexibility be clearly raised or improved compared to systems before option was made for the use of combined optics. Primary technical indices reached or exceeded required engineering targets. Performance, mounted and in actual use, reached, and in certain areas, even exceeded the levels of the same type of range finding devices inside and outside China. /15

II. BASIC OPERATING PRINCIPLES

As is shown in Fig.1, laser beams coming reflected back from ranged targets and visible light beams go through common objectives in sequence (1). After a common image rotating lens (2), parallel beams are incident on cubic prism (3). From the cubic prism spectral plane, the $\lambda = 1.06\mu m$ laser beams are transmited through. After being filtered through narrow band filter (4), detector matching lens (5) will converge the beams. Then, after the size of the field of view is controled by reception field of view diagphragm (6), they arrive at the light sensitive surface associated with silicon avalanche photoelectric diode detector (7). Photoelectric conversion is carried out, producing the echo signal required for range finding. It is possible to see that, after light goes through the cubic prism and is split, light path reflection deflection is 90°. After going through visible light aperture diaphragm (8) to control the actual aperture, there is incidence on visible light image rotation lens (9). This lens set will form images on graduated scale (10). It then passes through eyepiece set (11). It enters human eyes at the location of exit pupil (12), observing and sighting on targets.

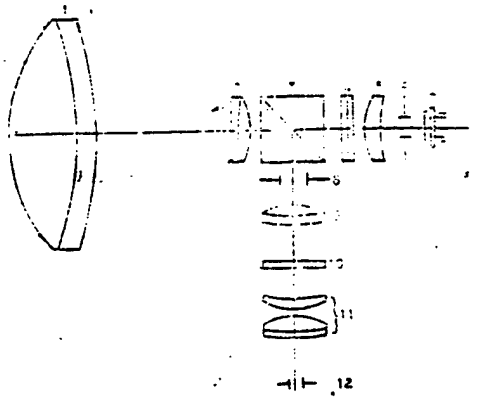

Fig.1 Combined Reception and Aiming Optical System

III. PRIMARY OPTICAL PERFORMANCE INDICES

1. Reception wave length: λ=1.064μm; 2. Effective aperture diameter: D(illegible)=80mm; 3. Reception field of view: θ(illegible)=2mrad; 4. Interference optical filters: W0.5=33A and To$\geq$0.6; 5. Reception system transmission rate: TJ(illegible) $\geq$ 0.4; 6. Spectral method: reflected visible, transmited 1.064μm; 7. Aiming multiple rate: Γ=18"-15"; 8. Observation field of vision: 2ω=2(illegible); 9. Discrimination rate: α=3''-4''.

IV. OPTICAL SYSTEM PARAMETER DETERMINATION

1. Determination of Reception Optical System Focal Length f'.

From the light path shown in Fig.1--based on Gaussian

optical principles--the reception light path system focal length is

$$f_1' = f_{11}' \cdot f_{31}' / f_{21}' \tag{1}$$

In the equation, f1J' --common use objective set focal length; f2J'--common use image rotation set focal length; f3J'--detector matching lens focal length. The relationship of system focal length and field of view is

$$f_1' = y' / \theta_2 \tag{2}$$

y' is ideal faculae diameter on detector light sensitive surfaces, that is, reception system image line viewing field.

$$y' = d - (\Delta y_1 + \Delta y_2 + \Delta y_3) \tag{3}$$

In the equation, d is detector light receiving surface diameter;

Δy1 is residual aberration diffusion; Δy2 is installation correction error amount; Δy3 is other influencing quantities.

Assuming Δy1 = 0.05mm, Δy2 = 0.15mm, Δy3 = 0.1mm, it is already known that θ(illegible) = 2mrad, and d = 0.8mm. Substituting into equations (2) and (3), one solves for the system focal length f(illegible)'= 250mm. /16

As far as the determination of f1JD' is concerned--considering aberration designs and optical system lengths when option is made for the use of dual bonding lenses--assume

D1/f1JD' = D1 • NF1 = 80x3=240mm.

With regard to the determination of f2JD' and f3J'--giving consideration to such factors as the possibility of being able to reach NF2 values associated with detector matching lenses NF3 and common use image rotation lens sets themselves as well as spectral prism aperture diameters and so on--adopt f2JD'as 35mm. Then, from equation (1), solve for f3J' = 36.458mm.

2. Reception System Viewing Field Diaphragm Positions and Aperture Diameters

From the relationships shown in Fig.2, one gets

$$d_1 = y' + \frac{D_3 - y'}{f_3'} \cdot l \tag{4}$$

Take D3=15 and l=3 as well as the relevent parameters and substitute in to obtain diaphragm diameter d1 = 1.693mm.

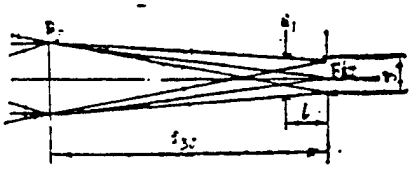

Fig.2

3. Determination of Aiming System Performance Parameters

Aiming objective lens optical systems are composed of common use objectives, common use image rotating lenses, visible light image rotating lenses, and cubic prisms. Because the property parameters of two common use lens sets are all already determined, therefore, the objective lenses in question only determine performance parameters associated with visible light image rotation lens sets. Indices give aiming system magnification power rates of $\Gamma=15°$. Giving consideration to focal lengths of ordinary eye piece sets, viewing fields, and the status of optical structures, the matching magnification rates associated with the two image rotation lenses are thereby determined. The system in question was initially fixed as $\beta D1 = f1D'/f2JD' = 1$, that is, $fDi' = f2JD' = 35mm$. After that, appropriate adjustments are then made in aberration design phases. In this way, aiming objective lens system focal length

$fD' = f1JD' \cdot \beta D1 = 240mm$. In equations, $fD1'$ is visible light image rotation lens set focal length.

Eye piece set focal length $f2D' = fD'/\Gamma$ (5)

Substituting in data, one obtains $fD2' = 16mm$.

Taking the parameters described above and applying systematization, after fixing corresponding aperture diameters for various optical sets, they are set out in Table 1.

4. Determing Optical System Initial Structural Parameters

On the basis of various optical unit performance parameters associated with optical systems as well as structural forms, use is made of p, w, and c methods to solve for initial structural parameters of various optical units r, n, and d or option is made for the use of ready made optical unit structural parameters. After systematization, they are inputed into computers to carry out design alterations.

Table 1

Optical Set	Focal Length	Corresponding Aperture Dia.	Model
Reception System	250.00	1:3.125	
Common Use Objective	240.00	1:3	Dual Bonding
Common Use Image Rotation Lens	35.00	1:2.05	Dual Bonding
Detector Lens	36.485	1:2.15	Positive Curved Moon Shape
Aiming Objective	240.00	1:4.36	4 Sets 8 Units
Aiming Image Rotation Lens	35.00	1:2.05	Dual Bonding

Ocular 16.00 1:1.43 2 Sets 3 Units

/17

V. SPECTRAL METHODS

As is shown in Fig.1, the spectral lenses in question are utilized under conditions where angles of incidence are 45°. The objective is thought of in terms of obtaining reflected light beams and transmited light beams which are perpendicular to each other in two beams of light of different wave lengths. In order to realize this type of beam splitting objective, it is possible to opt for the use of forms as shown in Fig.3.

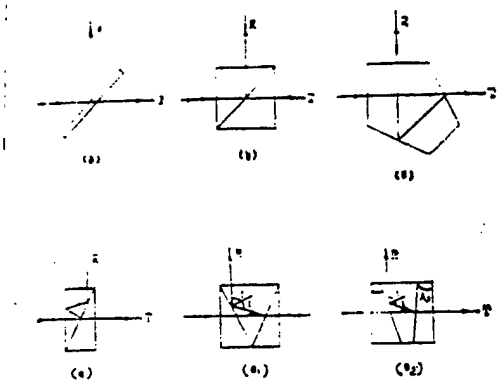

Fig.3 Spectrum Forms

In terms of form, the results obtained by the various types of spectral methods shown in Fig.3 are the same. In reality, due to the fact that polarization creates severe heterodyne halos, differences in results are still very great. As a result, when

designing spectral lenses, one should make strict verifications with regard to light path spectral characteristics, diaphragm system designs, and film plating techniques. Option is then made for the use of forms of spectral lens.

As far as parallel flat plate glass spectral lenses are concerned, in light paths, there is an oblique angle I relative to light axses (light rays), as shown in Fig.4. In that case, light axses (or light rays) will shift laterally D

$$D = t\cos I(\tan I - \tan I')$$

$$= t\sin I\left[1 - \left(\frac{1-\sin^2 I}{n^2-\sin^2 I}\right)^{\frac{1}{2}}\right] \qquad (6)$$

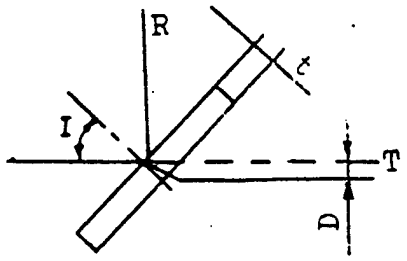

Fig.4

If angle I is very small, then, the equations above simplify to become:

$$D = \frac{tI(n-1)}{n} \qquad (7)$$

In equations, I is the angle of incidence of light rays on the first surface. I' is the angle of radiation outward of light rays on the second surface. n is the index of refraction of the glass material. As a result, when parallel flat plate spectral lenses are applied in combined laser reception and aiming optical systems, if T transmits a single wave band with $\mu = 1.06\mu m$, then, it is necessary to opt for the use of relatively complicated detector matching lenses in order to add improvements. If T transmits visible light wave bands, it is then necessary to do a good job of resolving light beam deviations and chromatic dispersions.

As far as prism spectral lenses are concerned, one of the important principles in design is that, as angles of incidence of light beams in prisms are reduced, the influences of polarization are thereby reduced--for example, the forms shown in Fig.3c and 3d. Opting for the use of composite prism compensation methods, selecting for use, at the same time, low index of refraction glass and applying equivalent concepts to search out diaphragm systems associated with small polarization effects is a very effective method of eliminating polarization--for example, two types of prism compensation spectral forms shown in Fig.3e. In this type of spectral form, if T transmits visible light, it is also necessary to consider eliminating chromatism. When use is made of prism combinations possessing the two vertex angles described below, it is possible to obtain prism sets eliminating chromatism.

$$A_1 = \frac{\theta v_1}{(n_1 - 1)(v_1 - v_2)} \tag{8}$$

$$A_2 = \frac{\theta v_2}{(n_2 - 1)(v_2 - v_1)} \tag{9}$$

If T transmits light associated with $\lambda = 1.06\mu m$, it is necessary to consider center wave length light beams not being able to have deviations. At this time, vertex angles of prism combinations are:

$$A_1 = \frac{v_1 v_2 \theta}{(n_1 - 1)(v_2 - v_1)} \quad (10)$$

$$A_2 = \frac{v_1 v_2 \theta}{(n_2 - 1)(v_2 - v_1)} \quad (11)$$

In equations, A1 and A2 are prism vertex angles associated with the first unit and the second unit. v1 and v2 are chromatic dispersions associated with prism materials and inverse proportions of the first unit and the second unit. As far as visible light is concerned, they are called Abei (phonetic) numbers, that is, v = (nD-1)/(nF-nc).

Using knowledge associated with the geometry of optics, it is easy to derive the conditions which must be satisfied in designing this type of compensation spectral prism:

$$A_1 + A_2 = 45° \quad (12)$$

$$I = 45° + A_2 \quad (13)$$

$$A_1 < I_c \tag{14}$$

$$I > I_c \tag{15}$$

In equations, Ic is the critical angle when prisms produce full reflection.

Finally, in accordance with Sinieer's (phonetic) Law, light ray trace corrections are carried out with regard to compensation combination prisms.

Fig.3b cubic spectral prism design results show performance as in Fig.5.

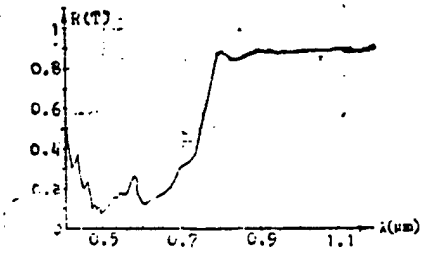

Fig.5 Reverse Charactersitics Associated with Cubic Prism Spectra Transmiting Visible 1.06μm

VI. ABERRATION DESIGN

During aberration designs associated with the combined optical systems in question, the author starts out from the properties of the two types of operations--laser reception and visible light aiming. At the same time, consideration is given to installation check methods in order to handle system aberrations.

1. Aberration Treatments Associated with Common Use Lens Sets

Taking initial structural parameters associated with common use objectives and common use image rotation lens sets and inputing them into computers, aberration corrections are respectively carried out. Not only is it necessary to take the three types of colored light aberrations D, F, and C and correct them to within general telescope objective aberration tolerances. It is also necessary to make 1.06μm light aberrations satisfy requirements. Option is made for the use of adaptation method self-balancing procedures, correcting F, D, and C aberrations first. Index values only require control. Full aperture diameter spherical aberration LA'index values are 0.03. As far as axial chromatism associated with aperture diameters is concerned, OSC' index values are 0.0002. Other chromatism index values are all filled in to be 0. Self-balancing aberration variable parameters are radii r and obverse lens thickness. Invariable parameters are auxilliary lens thickness, index of refraction, and focal length. Boundary conditions are guaranteed and high order amounts of spherical aberration are controled. After visible light aberrration tolerances are satisfied, option is again made for the use of direct output diffusion circle programs to carry out aberration calculations with regard to 1.06μm light.

As far as matching between two common use lens sets is concerned, there are dual wave band focal aberration problems. The author makes use of visible light as the standard, letting objective visible light image area focal point F1D' and image rotation lens visible objective area focal point F2D coincide. In this way, with regard to light beams going through image rotation lenses and being trransmited out to arrive at cubic spectral prisms, visible light is parallel beams. With respect to 1.06μm, because objective lens image area focal points F1J' are located within one multiple of the focal length of image

rotation objective lens area focal point F2J, therefore, 1.06μm light beams associated with going through image rotation lenses and being transmited out to cubic prisms become divergent light beams. Taking this a step further, after going through prism spectral transmission, it is still divergent light beams which are incident on narrow band interference optical filters. For this reason, it is necessary to make a calculation of whether or not the influences of divergent light beams on the performance of optical filters are permissible. This is very important with regard to optical interference filters which opt for the use of wide bands that are around 20Å. Divergent light beam angles make marrow beam optical interference filter peak value wave length shift ranges be: /19

$$\Delta\lambda = \frac{\phi^2}{2n'} \lambda_c \qquad (16)$$

In equations, n' is coating medium equivalent index of refraction. ϕ is divergent light beam semiconical angle. λ_0 is optical filter peak value wave length.

Within shift ranges, various optical filter parameter changes are:

Peak value wave length: $\lambda_\phi = \lambda_0 - \Delta\lambda/2$ (17)

Half band width: $W_\lambda = \sqrt{W_{0.5}^2 + \Delta\lambda^2}$ (18)

Peak value transmissivity: $T_\phi = \frac{W_{0.5}}{\Delta\lambda} \tan^{-1} \frac{\Delta\lambda}{W_{0.5}}$ (19)

In equations, W0.5 is optical filter half power location band width.

The objectives of handling aberrations in this way with regard to two common use lens sets are, on the one hand, that, during mounting corrections, it is convenient for the use of visible light checks and corrections. So long as visible light mounting correction checks reach design levels, laser reception light paths must also lie in design performance configurations. On the other hand, image rotation and parallel light spectra are not only arrived at. It is also possible to make narrow band interference optical filters be placed into optimum operational performance.

2. Reception System Aberration Handling

Taking common use objective lens, common use image rotation lens, and cubic prism residual aberrations and substituting into P and W methods--after solving for detector matching lens initial structure parameters--structural parameters associated with the entire system are then taken and inputed into computers to carry out system aberration balancing. It is possible to alter

parameters for detector matching lenses r, d, n, and f. From the principles of equation (1), adjustments are made of different matching multiple rates associated with f3J' and fJD' in order to regulate system focal length fJ'. Thus, image plane light faculae size is controled. At the same time, optimum image surfaces are sought, evaluating their advantages and disadvantages. So long as the sum of aberration diffusion and image area linear viewing field is smaller than the diameter of detector surfaces receiving light, that will do. There is no need to make specific analyses with regard to various types of aberration capacities. Giving consideration to assembly errors, it is possible, on the basis of actual situations, to match faculae and the light receiving surfaces of detectors, leaving a certain appropriate margin.

3. Aiming System Aberration Handling

Aiming system aberration handling and conventional telescope design are the same. The various lens sets in front of graduated scales are seen as a complex lens. Taking the structural parameters and inputing them into computers, alterations are made of various parameters associated with visible light image rotation lens sets. Aberration balancing is carried out with regard to combined lens optical systems. Finally, together with the same eye piece set, structural parameters associated with the entire aiming system are taken and inputed into computers. Besides that, input is made of ideal optical systems without aberration, carrying out aberration calculations for the entire system. Various aberrations on ideal system focal planes, which computers output, are nothing else than the various aberration values associated with the aiming systems in question.

VII. DESIGN RESULTS

Table 2 Optical Properties

Reception System		Aiming System	
Useful Diameter:	80mm	Objective Focal Length:	269.65mm
Viewing Field Angle:	2mrad	Relative Aperture:	1:4.3
System Focal Length:	210.1584mm	Magnification Rate:	18.4x
Detection Plane Optical Faculae Diameter:	0.441mm	Viewing Field Angle:	2°
System Transmissivity:	0.422	Exit Pupil Diameter:	3mm

Reception Light Wave Band Width: 33Å

Discrimination Rate: 3"

/20

Table 3 Various Properties of Optical Sets

Nomenclature	f'	LF	LF'	ϕ Effect	External Form	d	Form
Common Use Objective	269.65	-269.03	257.40	80.00	84.70	20.00	Double Bond
Common Use Image Rotation Lens	37.66	-33.75	35.97	18.00	20.00	8.30	Double Bond
Spectral Prism	Reflects Visible	Transmits Visible	1.064	18.00	Aperture 20x20	20.00	Dual Right Angle
Optical Interference Filter				18.00	30.15	4.20	Double Bond
Detector Lens	28.68	-29.36	25.80	17.00	19.00	3.80	Single Crescent
Visible Light Image Rotation Lens	37.66	-35.97	33.75	18.00	20.00	8.30	Double Bond
Graduated Scale	Ruled Values	1mrad		10.00	15.00	2.00	Single Piece
Ocular	14.64	-13.44	11.33	17.00	19.00	7.30	Two Set Two Unit

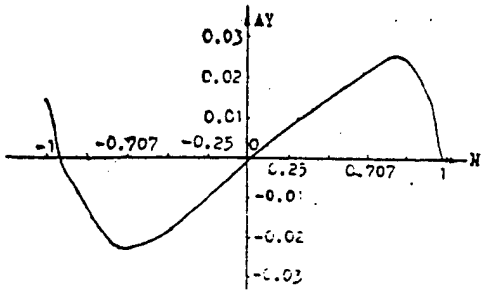

Fig.6 Reception System Aberration (1 Viewing Field). In Fig., Δy' Is Aberration Dispersion. H Is Light Passing Aperture

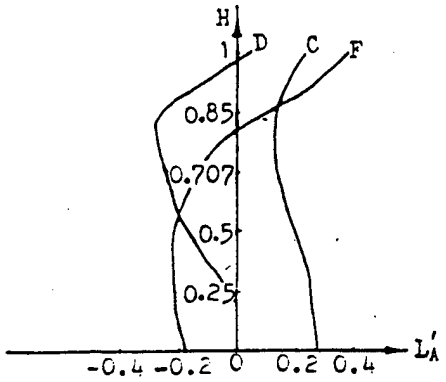

Fig.7 Aiming System Spherical Aberration Chromatism Curves

REFERENCES

〔1〕 李景镇主编，《光学手册》，陕西科学技术出版社，1986年，第155～157页。

〔2〕 《四川激光》，1980年，第3期，第5～10页。

〔3〕 《电光系统》，1986年，第3期，第53～58页。

NAIC-ID(RS)T-0150-96.2 /27

INVESTIGATION OF CO2 LASER PARAMETRIC UPCONVERSION

Zhong Ming Han Kai

Translation of "CO2 Ji Guang Can Liang Shang Zhuan Huan De Yan Jiu"; Laser Technology, Vol.13, No.1, pp 27-30

ABSTRACT

This article reports for the first time on research results associated with CO2 laser light upconversion in AgGaS2 crystals into near infrared radiation. Using SPD-052 avalanche photodiode detectors, equivalent noise power (NEP) of ~3.8x-8W and normalized detectivity of $(D_\lambda) \sim 10^{10} cmHz^{1/2}W^{-1}$.

were obtained. The power conversion efficiency of type II noncolinear phase matching is estimated to be 10%.

I. INTRODUCTION

Making use of frequency upconversion to detect CO2 laser light is still a new technology which is in the midst of exploration. The theory was put forward early in 1962 by Amrstrong and Bloembergen [(illegible)]. For over 20 years, people have right along made various types of efforts to improve upconversion efficiencies. In 1977, W. Jantz and P. Koidl opted for the use of type I colinear 90° phase matching, obtaining 40% quantum conversion efficiencies [2(illegible)]. In the same year, S.A. Andreev and others opted for the use of type II noncolinear phase matching, obtaining 9% power conversion efficiencies [3]. In 1979, E.S. Voronin and others opted for the use of two stage conversion, regulating Q focus pumps and obtaining 24% conversion efficiencies [4]. In 1982, T. Itabe and others reported for the first time on an actual detection system associated with a CO2 10.6μm pulse laser radar unit [5] used in detecting radar back scattering (illegible) signals associated with atmospheric sols outside several kilometers. Estimates were that detection sensitivities were two orders of magnitude higher than direct observation, reaching 1012 cmHz1/2 W-1 . Inside China, there are also people who have developed work in this area (illegible).

/28

Comparing the use of frequency upconversion to detect CO2 laser light with direct detection, the most important advantage is that there is no need for low temperature cooling. It is possible to detect at normal temperatures. Speaking with regard to engineering users, this undoubtedly possesses extremely great attaction. The authors believe that making use of frequency upconversion to detect CO2 laser light has existing in it three main technological difficulties. One of them is to obtain high conversion efficiencies associated with conversion from infrared signals to sum frequency signals. The second among them is technologies assocciated with filtering out of pump light. The third among them is synchronous pump problems associated with pulse infrared signals.

This article reports on research results associated with the conversion of CO2 laser light in AgGaS2 crystals into near infrared radiation. In theoretical terms, we start out from three wave coupling equations, deriving a unified expression associated with conversion efficiency η as well as pump light intensity Ip and wave vector difference ΔK. In experiments, option is made for the use of type II noncolinear phase matching.

In conjunction with this, option is made for the use of pump light filtering technologies associated with polarization prisms,

shine diaphragms, and optical interference filters in combination, obtaining good results.

II. POWER CONVERSION EFFICIENCIES

Frequency upconversion is nothing else than taking signal waves associated with "low" frequency ωir and strong light beams associated with frequencies that are ωp and mixing the frequencies together in crystals. Making use of the parameter interaction in crystals, it is possible to take "low" frequency ωir waves and convert them into "high" frequency ωup waves. Among these, one has ωir + ωp = ωup.

Setting out from three wave interaction coupling wave equations [8], assume that pump dissipation can be ignored in calculations. In conjunction with that, assume that absorption losses are zero. Then, it is possible to derive power conversion efficiencies

$$\eta = \frac{P_{up}(l)}{P_{ir}(0)} = \frac{\omega_{up}}{\omega_{ir}} g^2 \frac{\sin^2 \sqrt{(\Delta K)^2 + g^2} \cdot \frac{l}{2}}{\sqrt{(\Delta K)^2 + g^2}} \tag{1}$$

In equations,

$$g^2 = \frac{2\omega_{ir}\omega_{up} d_{14}^2}{\eta_{ir}\eta_p\eta_{up}} \left(\frac{\mu_0}{\varepsilon_0}\right)^{3/2} I_p \tag{2}$$

$$\Delta K = K_{up} - K_{ir} - K_p \tag{3}$$

Subscripts up, ir, and p stand, repsectively, for various quantities associated with sum frequency, infrared signals, and pump light.

If ΔK=0, then equation (1) becomes

$$\eta = \frac{P_{up}(l)}{P_{ir}(0)} = \frac{\omega_{up}}{\omega_{ir}} \sin^2 \frac{gl}{2} \tag{4}$$

This equation describes the relationships between conversion efficiencies and pump light intensities and is consistent with conclusions (illegible) references.

If ΔK >> g, that is, when pump light intensities are relatively weak, then equation (1) becomes

$$\eta = \frac{\omega_{un}}{\Delta\omega_{i:}} g^2 \, l^2 \, \mathrm{sinc}^2\left(\Delta K \cdot \frac{l}{2}\right) \tag{5}$$

This equation describes the relationships of conversion powers and wave vector differences (illegible). It is possible to see that, under conditions where pumps are weak, reducing ΔK is the key to obtaining high conversion powers. /29

III. EXPERIMENTAL SYSTEM

In the experiments in question, we opt for the use of type II noncolinear phase matching methods.

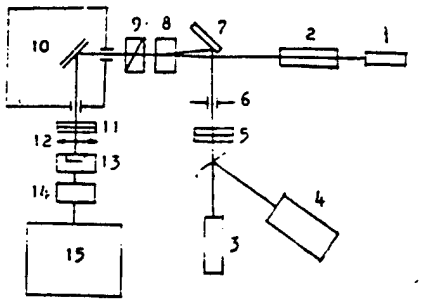

Fig.1 Frequency Upconversion Experimental Apparatus Schematic 1. He-Ne Laser 2. d:YAG Laser 3. CO2 Laser 4. Spectral Line Analyzer 5. Germanium Attenuator Plate 6. Shutter 7. Gold Plated Reflector Surface 8. AgGaS2 Crystal 9. Nicol Prism 10. Diaphragm Monochrometer 11. Optical Filter Unit 12. Converging Lens 13. Silicon Avalanche Photoelectric Diode 14. Wide Band Magnifier 15. Oscillascope

The operating principles are that, within cavities, Nd:YAG lasers fitted with polarization components output 1.06μm horizontally polarized light (λp). Stable frequency polarized CO2 lasers output 10.6μm vertically polaized light (λir, the wave length is monitored by CO2 spectrograph). The latter goes through gold plated reflector reflection and 1.06μm pump light makes use of quasi colinear methods to enter into AgGaS2 crystals to carry out nonlinear interactions (the included angle between

the two is 0.5°±0.1°), obtaining near infrared vertically polarized sum frequency light associated with

$$\lambda_{..} = \frac{\lambda_{.} \lambda_{1.}}{\lambda_{.} + \lambda_{1.}}$$ = 0.96μm. By Nicol prisms, diagphragm monochromaters and optical filter units filter out pump light. After that, sum frequency signals are received by SPD-052 silicon avalanche photoelectric diodes. Following amplification, they are displayed by CS-2100 model oscilloscopes.

IV. EXPERIMENTAL RESULTS

1. Power Conversion Efficiency Estimations

From equation (1), it is known that power conversion efficiencies

$$\eta = Pup(1)/Pir(0)$$

In the equation, Pir(0) can be directly read out from dynamometers. Pup(1) then needs to be estimated by the methods set out below. As far as degrees of response of avalanche photoelectric diodes to 0.96μm wave lengths are concerned, we carry out direct calibration. Moreover, shining efficiencies of shining diaphragms with regard to 0.96μm wave lengths are then calculated on the basis of the two stage shining efficiencies associated with 5461Å. Transmissivities of lenses and optical filters with respect to 0.96μm are determined by UV-365 model photometers. On the basis of the various data above, it is possible to estimate power conversion efficiencies in nonlinear crystals to be 10%.

In our experiments, pump light power density is 5.9x106cm-2. The principal causes for experimental power conversion efficiency ηexp being lower than theoretical calculated values ηth = 20% are: 1. crystal surface reflection losses with regard to infrared signals 2. crystal absorption 3. bad beam quality in pump light 4. crystal optical quality not uniform.

2. Normalized Detectivity D^*_λ

Normalized detectivity can be represented as [10(illegible)]

$$D^*_\lambda = \frac{(A_D B)^{1/2}}{P}\left(\frac{V_S}{V_N}\right) \qquad (6)$$

In equations, A (illegible) is detector light sensitive surface (cm2). B is detector system band width (Hz). P is incident radiation power. (Vs/Vn) is signal voltage ratio (noise is measured in band width B). /30

In our experimental apparatus, AD is obviously beam cross section areas associated with nonlinear crystal surfaces with pump light incident on them. It is possible to make use of 1.06μm conversion displays for measurements. Power P is measured

by LPE-1A dynamometers. Vs and Vn are read out by CS 2100 oscilloscopes. Because band widths associated with magnifiers and avalanche photoelectric diodes are 40MC in all cases, but oscilloscope band widths are 100MC, B=40MC is, therefore, adopted. Calculating from equation (6)

$$D_\lambda^* \sim 1 \times 10^{10} \text{ cmHz}^{1/2} \text{ W}^{-1}$$
$$\text{NEP} \sim 3.8 \times 10^{-8} \text{W}$$

3. Noise Characteristics

Functioning as a detection system, noise is unavoidable. Reference [11] sets out seven types of noise sources associated with upconversion detection. In conjunction with this, it is believed that pump background noise is the most important noise. In our experiments, pump background noise achieved full suppression. Moreover, it is possible to expect to achieve further improvements. As a result, we believe the most important noise associated with detection systems is still detection component noise and magnifier noise. Work related to this area is still continuing to be carried out.

V. CONCLUSION

As far as our work is concerned, seen from the view of this detectivity index, the level of practical utilization has already been achieved. During Nd:YAG pump laser dye Q adjustment output (pulse 8ns), the noise equivalent power (NEP) and normalized detectivity achieved by detection systems as a whole were 3.8x10-8 and D_λ^* ~ 1010cmHz1/2W-1. With regard to this index, it is slightly lower than HgCdTe direct detection levels. If, in the optimization of utilizations associated with vapor plated infrared increased transmission coatings and avalanche photoeletric diodes, such measures as difference amplification are adopted in circuits in order to eliminate pump noise, it is possible to expect to have improvements on a relatively large scale. However, synchronization pump problems associated with pulse infrared signals still have not been effectively resolved. We plan to opt for the use of weak focusing and long pulse pumps in order to resolve this problem.

AgGaS2 crystals used in experiments were supplied by Stanford University Professor R.L.Byer. The authors express their heartfelt gratitude.

(Brief introduction of authors: Zhong Ming. Male. Born May 1957. MS. Engaged in nonlinear optics and laser detection (illegible) technology research.)

REFERENCES

〔1〕 Phys. Rev. , 1962, Vol. 127, P. 1918.

〔2〕 Appl. Phys. Lett. , 1977, Vol. 31, P. 99.

〔3〕 Sov. J. Q. E. , 1977, Vol. 7, No. 3, P. 366.

〔4〕 Sov. J. Q. E. , 1979, Vol. 8, No. 9, P. 1145.

〔5〕 Appl. Opt. , 1982, Vol. 21, No. 13, P. 2381.

〔6〕 《激光》, 1981年, 第8卷, 第11期, 第30页.

〔7〕 《激光杂志》, 1986年, 第7卷, 第8期, 第8页.

〔8〕 A. Yariv, Quantum Electronics, New York, Wiley. 1975. P. 418.

〔9〕 F. Zernike, J. E. Midwinter, Applied Nonlinear Optics, New York, Wiley, 1973. P. 44.

〔10〕 R. J. 凯斯主编, 董培芝等译, 《光探测器与红外探测器》, 科学出版社, 1984年. 第56页.

〔11〕 Jap. J. A. P. , 1966, Vol. 5, No. 5, P. 389.

MEASUREMENTS OF THE BACKSCATTERING AND RETROSCATTER OF OPTICAL SURFACES AND HIGH REFLECTANCE MIRRORS

Kong Xianggui Feng Tiesun

Translation of "Guang Xue Biao Mian He Gao Fan She Jing San She Jiao Fen Bu Ji Fan Xiang San She De Ce Liang"; Laser Technology, Vol.13, No.1, pp 31-34

ABSTRACT

This article gives a type of measurement apparatus for measuring angular distributions of scattering for polished surfaces and high reflectance mirrors. In conjunction with this, it puts forward designs for accurately measuring the retroscatter.

I. INTRODUCTION

As far as scattering which is produced by surfaces with degrees of roughness far, far smaller than wave lengths is concerned, it is possible by various types of methods to make determinations [1]. One among these is angular distribution scattering measurement [2-4]. It is not only capable of solving surface height and autocorrelation functions associated with microscopic surface nonuniformities. It is, moreover, also capable of determining in an approximate manner surface retroscattering. Retroscattering is a key factor giving rise to locking phenomena produced by laser gyroscopes, and reducing laser reflection mirror retroscattering is even more important. At the present time, in China, use is normally made of integration sphere apparatus to measure scattering given rise to by surfaces. However, this type of method is only capable of giving overall results for scattering. It is, however, not able to give scattering associated with the angles inside certain small solids or certain directions. In particular, retroscattering associated with laser gyroscope reflectance mirrors is most important. In this article, the authors put forward a type of design for measuring scattering angular distributions. In conjunction with this, an improved design to measure retroscattering is put forward.

II. MEASUREMENT OF SCATTERING ANGULAR DISTRIBUTIONS

Experimental apparatus is as shown in Fig.1a and b. He-Ne laser 632.8nm spectral lines act as light sources. The output power is 1mW. Light passes through a polarizing plate K which is capable of adjusting the polarization direction. After that, SF wave filtering is done by spacial wave filters. Spectral lens Mp will divide the light into two beams. One beam is received by dynamometer P in order to monitor fluctuations in light intensity. The other beam, after passing through attenuation plate MA is incident on sample M. Attenuation plate MA is a high reflectance mirror. When light paths are adjusted, they are made to have an included angle with light axses in order to avoid back and forth reflection in light paths. Sample M is placed on a turn table that is capable of rotating, making incident light able to shine on samples using different angles of incidence. Scattering light is received by a light transmiting optical fiber bundle F with a diameter of 5mm. The end surface is

approximately 120mm from the sample. The reception angle associated with the spacial solid formed is $\Delta\ \Omega$ = 1.1x10-4 rad. One end of fiber optic bundles is installed on a degree plate which is capable of rotating. With rotation of the degree plate, it is possible to measure out light scattering associated with directions at different angles. The other ends of fiber optic bundles are connected to photon counting device PC. Photon counting devices are weak signal detectors associated with linear ranges that are relatively wide and detectivities that are quite high. Their linear ranges are numbers of photons from 10-107. Noise fluctuations are smaller than 20 photons in number. Option is made for the use of multiple iterations of measurements. It is possible to eliminate the influences of noise fluctuations. In experimental systems, reflected and transmited light produced by all other components is absorbed in all cases by dark cases c1, c2, c3, and c6, suppressing as much as possible background noise associated with instruments. Measurements revealed that instrument background light noise is only around 10 photons in number.

In order to measure minutely small scattering as well as eliminating influences associated with optical component transmission and reflection in instruments, it is necessary to carry out calibration and measurements with regard to instrumentation, as is shown in Fig.1b. At this time, an attenuation plate MB, with an already known attenuation coefficient that is T, is placed behind attenuation plate MA, selected to go to the sample. Optical fiber end surfaces are taken and directly aligned to transmited light.

On the basis of Fig.'s 1 a and b, it is easy to get the internal retroscattering coefficient associated with $\Delta\Omega$ as

$$S_e\Big|_{\Delta\Omega} = \frac{N_m \times P_c \times T}{N_c \times P_m} = \frac{I_r}{I_e} \qquad (1)$$

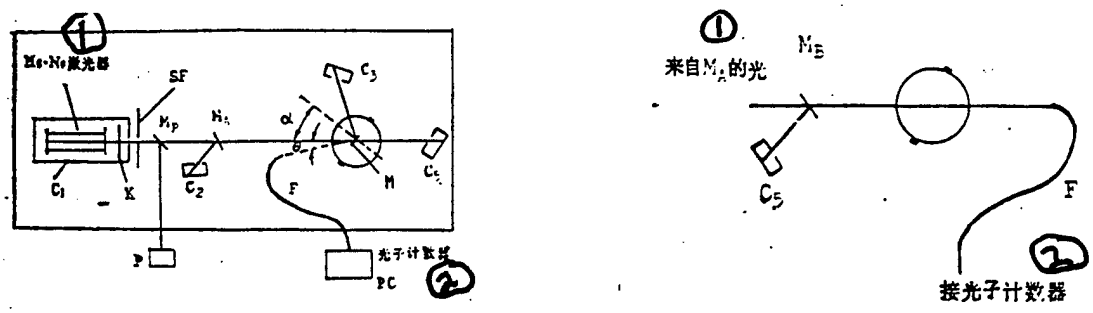

Fig.1 Scattering Angular Distribution Measurement Apparatus and Process a. Scattering Angular Distribution Measurement Apparatus

Key: (1) Laser (2) Photon Counter
b. Calibration System

Key: (1) Light Coming from MA (2) Connection to Photon Counter

In equations, I(illegible) is the scattering light intensity associated with the interior of the angle $\Delta\Omega$. Io is incident light intensity. N(illegible) and P(illegible) correspond to photon couunting device and dynanometer measurement values in Fig.1a. NC and Pc correspond to photon counter and dynamometer measurement values in Fig.1b. Obviously, scattering parameters are barely related to transmissivities T associated with attenuation plate MB. Moreover, they are not dependent on the reflection and transmission properties associated with attenuation plate MA, spectral lens Mp, and fiber optic bundle F. So long as it is possible to accurately measure T, it is then possible to accurately measure scattering coefficients. Theoretical error can reach 5%. On the basis of equation (1), it is possible to obtain this. The designs in question are capable of measuring scattering coefficients smaller than 10-10. However, it is necessary to pay attention to guaranteeing--when doing all measurements--that fiber optic curve forms should, as much as possible, be in line with fiber optic curve forms during calibration measurements.

Table 1 gives four samples and measurement results associated with four different angles. Among these, two samples are polished substrates which have not yet been plated with high reflectance coatings. In reality, their scattering eminates from the two front and back surfaces. If it is roughly acknowledged that the reflection coefficients associated with the two surfaces are basically the same--when polarized light is parallel to

polarized light associated with incident surfaces--going through calculations, the effects produced in association with the back surface can be ignored in calculations.

After calculating large numbers of scattering coefficients for different angles, it is possible to estimate the quality of these optical surfaces [4(illegible)]. We will not discuss this in more detail here. /33

From the results of Table 1, it can be seen that, compared to results in reports outside China, the scatterings produced by substrates and high reflectance mirrors are higher by two and even three orders of magnitude. Besides this, scatterings associated with high reflectance mirrors are almost primarily dependent on optical substrates. As a result, the obtaining of high quality optical substrates is very important.

Table 1 (Incidence Angle α=30°, Light Polarization Direction Parallels Incidence Surface T=2.1%)

	S, | sr			
(1) 样品	$\theta = 8°$	$\theta = 18°$	$\theta = 28°$	$\theta = 38°$
(2) 基片一	6.8×10^{-7}	8.4×10^{-7}	4.0×10^{-7}	2.5×10^{-7}
(3) 基片二	3.2×10^{-6}	2.8×10^{-6}	2.5×10^{-6}	1.0×10^{-6}
(4) 高反镜一	1.0×10^{-6}	1.2×10^{-6}	8.0×10^{-7}	7.0×10^{-7}
(5) 高反镜二	1.6×10^{-6}	1.5×10^{-6}	1.1×10^{-6}	6.9×10^{-7}

Key: (1) Sample (2) Substrate I (3) Substrate II (4) High Reflectance Mirror I (5) High Reflectance Mirror II

III. MEASUREMENTS ASSOCIATED WITH RETROSCATTERING

Up to the present time, there has not yet been an apparatus for accurately measuring retroscattering. What is called retroscattering refers to scattering which is in a direction completely opposite to the direction of incident light. In actual situations, it is difficult to measure scattering associated with this direction. Normally, it is only possible to

measure scattering which has a certain included angle with this direction. It is very difficult to have this included angle smaller than 6°. Making use of the results obtained in experiments, one gets an approximation of scattering at 0°, that is, retroscattering. However, in directions in the vicinity of reverse, changes in scattering are capable of being very abrupt. Thus, there is a need to carry out accurate measurements with regard to these. The authors put forward the experimental apparatus in Fig.2. Spectral lens Mp1 is placed between sample M and attenuation plate MA. Fiber optic bundle end surfaces are accurately adjusted, receiving retroscattered light. Instrument calibration methods are similar to situations during angular distribution scattering measurements.

However, MP1 will also produce scattering. Therefore, it requires that there be good quality plated coatings. Going a step further, here, two iterations of measurements are adopted in order to completely eliminate scattering produced by MP1, as is shown in Fig.'s 2 a and b. The first step is sample placement. The second step is changing samples into dark cases. Backscattering produced by sample M is /34

$$S_{\cdot\cdot} = \frac{(N_{\cdot}' - N_m P_{\cdot}'/P_m') T \times P_{\cdot}}{N_{\cdot} \times P_m' \times R} \qquad (2)$$

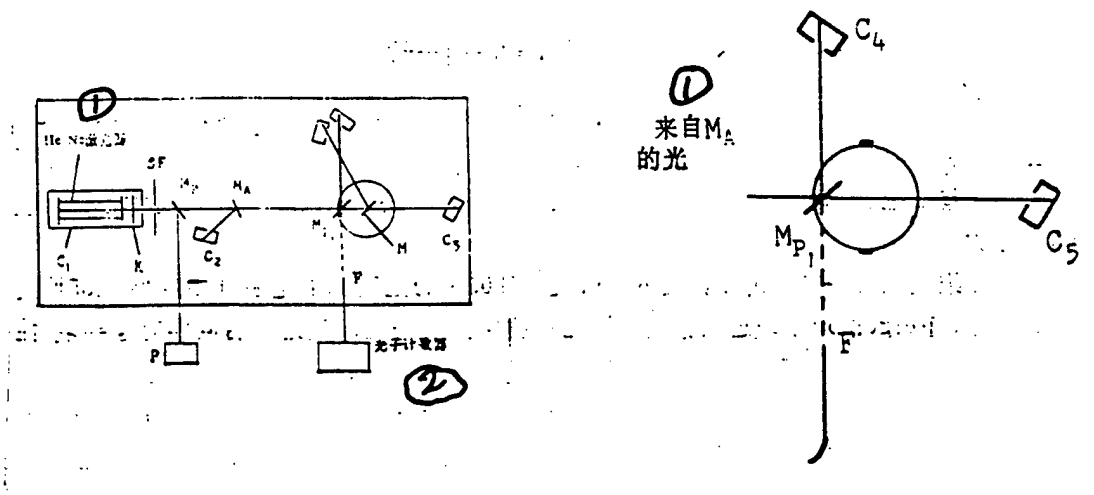

Fig.2 Retroscattering Measurement Apparatus
a. Measurement of Retroscattering Associated with MP1 and M
Key: (1) Laser (2) Photon Counter
b. Measurement of Scattering Given Rise to by MP1
Key: (1) Light Coming From MA

In the equation, Nm' and Pm' are photon counter and dynamometer

readings in Fig.2a. Nm and Pm are photon counter and dynamometer readings in Fig.2b. R is the reflection factor associated with MP1(illegible). With this apparatus, measurements were made of the retroscattering coefficients associated with two high reflectance mirrors. These were, respectively, 5.5x10-6 and 6.2x10-6. Results clearly show that they are far, far greater than $\theta = 8°$ values.

Comrade Zhou Jiulin provided high reflectance mirrors for experimental use. For this, we express our gratitude.

[Brief introduction of authors. Kong Xianggui. Male. MS. Presently a doctoral candidate specializing in the Qinghua University precision instruments department. The direction of his research is ring shaped laser gyroscopes, laser reflection scattering measurements, and so on. Feng Tiesun. See this publication, 1987, Vol.11, No.6, P.62.]

REFERENCES

(1) Appl. Opt. , 1984, No. 23, P. 3820.

(2) Proc. Soc. Photo-Opt. Instrum. Eng. , 1983, No. 384, P. 123.

(3) Proc. Soc. Photo-Opt. Instrum. Eng. , 1983, No. 384, P. 2.

(4) Appl. Opt. , 1984, No. 23, P. 3561.

NAIC-ID(RS)T-0150-96.4 /46

APPLICATIONS OF FIBER OPTIC TECHNOLOGY IN U.S. MILITARY FIELDS

Tan Xianyu

Translation of "Guang Xian Ji Shu Zai Mei Jun Shi Ling Yu Zhong De Ying Yong"; Laser Technology, Vol.13, No.1, pp 46-50

ABSTRACT

What this article primarily introduces is applications of U.S. fiber optic technology in the areas of military fiber optic communications, fiber optic guided missiles (FOG-M), guided torpedoes, launching of remote control aircraft, mine laying, and fiber optic sensors.

I. INTRODUCTION

As far as U.S. fiber optic technology is concerned, military use preceded civilian use. To a very great extent, civilian uses are driven by military uses. In recent years, the U.S. investment in military use fiber optic technology has increased by the year. In 1981, the U.S. investment in fiber optic technology (including miltary uses and civilian uses) was only 134.5 million U.S. dollars (in this, communications accounted for 34%, military and government departments accounted for 27%, control accounted for 27%, and other projects accounted for 12%) [1] (illegible). According to 1987 reports by the U.S. KMI company, during the five year period 1986-1990, the total investment used in fiber optic technologies was planned to approach or even exceed 1.7 billion U.S. dollars. In this, 1986 was 196.4 million U.S. dollars. 1990 was forecast to be 509 million U.S. dollars. In the five year period, the Army fiber optic guided missiles required 645 million U.S. dollars, and service communications required 214 million U.S. dollars. Air Force fiber optic gyroscopes required 162 million U.S. dollars, and service communications required 291-761 million U.S. dollars.

Navy antisubmarine weapons (ASW) required 80 million U.S. dollars, and service communications required 256 million U.S. dollars [3] (illegible).

Due to the unique advantages which fiber optics possess in and of themselves--for example, abundant raw materials, low light losses, safety and reliability, strong security characteristics, small volumes, light weight, not being subject to electromagnetic interference, resistance to chemical corrosion, and so on--they are very suitable for military applications. As a result, the U.S. military has introduced enormous manpower and financial resources into all areas of fiber optic communications and noncommunications realms--for example, fiber optic guided missiles (FOG-M), fiber optic sensors (including fiber optic gyroscopes), fiber optic guided torpedoes, launched remote control drones, as well as mine laying, and so on--achieving great progress.

II. FIBER OPTIC TECHNOLOGY USED IN MILITARY COMMUNICATIONS

/47

In order to adapt to bad combat environments, the U.S. Defense Department put forward stringent requirements with regard

to communications. They demanded sure communications and control without errors under any conditions. Due to the unique advantages possessed by fiber optics, it was possible to flexibly and reliably install fiber optic cable, fitting out fiber optic communications equipment used in the military. Therefore, the U.S. Navy, in 1973, installed an internal military use fiber optic communications system on the warship "Pebble City" (probably Chinese rendering of the meaning of a related original English name) [[273(illegible)]].

In the area of military use fiber optic communications, the U.S. is in the midst of building and has already handed over for utilization large scale military use optical communications projects, including the following.

1. Fiber Optic Long Distance Communications System (FOTS)

In July 1982, the U.S. Army Communications Electronics Command gave to the ITT company a design and development contract for long distance fiber optic communications systems FOTS (illegible) LH, managed by the Ft. Monmouth, New Jersey Electronics Communications Command. It was planned to opt for the use of 10,000km of optical cable and connection port equipment to replace the currently existing CX-11230 dual coaxial electric cable, completing communications contacts between battlefield and command locations (illegible) guaranteeing full tactical communications associated with army internal rear service bases. This system not only reduces weight 67%. Relay stations are reduced 80%. Moreover, information transmission capacities are also increased [illegible].

Beginning in 1983, the U.S. Army Electronics Communications Command and the Defense Department opted for the use of 10,000km of optical cable to replace coaxial electric cable. In South Korea, from Seoul to Pusan, 667km of tactical communications line were constructed in order to replace the original microwave lines. This fiber optic cable takes up little space. It is buried under the ground in conduit and does not easily suffer attack. The optical cable in question includes in it 12 optical fibers. Operating wave length is 1.3μm, transmiting information at 45Mb/s [6].

The U.S. Army and Air Force opted for the use of helicopters to lay optical cable in order to increase the combat power of mobile tactical strike units (for example, accelerating deployment of units). Fig.1 is the optical cable associated with the optical fiber tactical communications network in the process of being jointly laid by the U.S. Army and Air Force. This is one part of the planned composite service tactical communications

TRI-TAC (triservice tactical communications network). It is also possible through satellites to maintain contact between tactical airborne radars and air defense radars [2].

Fig.1 Schematic Diagram of the U.S. Air Force and Army in the Process of Using Helicopters to Lay Optical Cable. User Separation Distances Reach 10-20km. Communications Are Possible in All Cases. 1. Tactical Radio Communications Line 2. Tactical Airborne Radar and Air Defense Radar 3. High Speed Helicopter Laying 4. Secure Communications 5. Satellite Communications

2. TAOL 85 System

This is the maritime optical fiber communications system invested in by the U.S. Navy. It has currently already entered

into the full development stage. The system in question uses fiber optic transmission of digital information on a trunk line over a distance of 500-2000m in order to complete such functions as automatic tracking switching, target display, identification, classification, as well as estimates of indications and selection of weapons, and so on, overcoming extremely short limitations on range associated with electric cable transmission of data. Microwave equipment volumes are large, and there are such disadvantages as bad security characteristics [3].

The U.S. Navy's Ariadne project takes optical cable and lays it on the sea floor in order to collect ocean bottom ASW (antisubmarine weapon) information. At the present time, principal locations are in Greeland, Iceland, and the United Kingdom in ordr to monitor Soviet submarines from this location on the sea floor entering the high seas. In order to analyze data associated with the sea bottom, use is made of optical fiber sensors to connect to computers on the sea coast. This project initially opted for the use of 50km optical cable. At the present time, it is capable of reaching over 100km. Investment for the project in question is from the U.S. Defense Advanced Research Projects Agency (DARPA) and is under the direct orders of naval aviation and naval warfare systems. In 1987, it had already gone into the high technology demonstration phase. At the present time, it is designated tactical detachment 62702E naval warfare project. Fig.2 is a schematic diagram of the U.S. Navy's use of destoyers at sea to lay optical cable [273(illegible)]. In general, modernized destroyers are capable of carrying several thousand kilometer lengths of optical cable. Optical cable carried by two or three warships of this kind are then sufficient to do transoceanic laying, supplying good quality wide band width communication lines.

According to reports, the U.S. Navy is also putting stress on opting for the use of fiber optic technology to redo circuits internal to the AV-8BV/STOL (vertical and short distance take off and landing), used in order to transmit information associated with aircraft attacking approximately 6km and cruisers associated with naval cover approximately 2-3km [3(illegible)]. /48

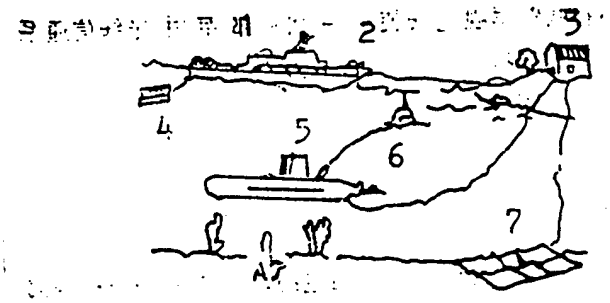

Fig.2 Schematic of U.S. Navy Using Destroyers at Sea to Lay Optical Cable 1. Electrical Cable Equipment 2. Interconnections on Submarines 3. Radio Communications Lines Capable of Crossing Oceans 4. Detector Radio Communications Lines 5. Tactical Radio Communications Lines 6. Concealed Laying 7. Passive Monitoring Net

3. In the Area of U.S. Forces Military Uses of Optical Fiber Communications, Systems Which Are Also Capable of Rapidly Laying Optical Cable from the Air in Unknown Areas

The optical fibers required by the systems in question are high strength and possess very high environmental resistance properties. The transmission speeds are 20-700kb/s. Line length is 0-3km. Operating temperatures are -40°C ■ +80°C. They have specialized small model optical transmission devices and reception devices. Transmission devices require optical powers transmited toward 50μm optical fiber core lines which are greater than 100μW. Operating voltages are 10V±2V. Optical output amplitude changes are lower than 50%. Reception devices matched to them operate under conditions associated with <10-5 BEH and peak value optical power lower than 10nW. The dynamic range is > 46dB. Typical current leakage is < 20mA. Electrical circuits associated with transmission devices and reception devices and optical conversion devices are mounted in all cases inside a 6.1mmx41.9mmx19.8mm small model metal case. This is able to

reduce deformations of optical fiber lead in lines and is convenient for high power coupling. The insertion pieces are capable of guaranteeing reliable operation in -40°C ■ +85°C and with part vibration and shock, thereby accelerating military applications of optical fiber technology [2].

For this reason, most recently, Valtec installed 147km of multiple mode optical fiber cable in the missile test center at California's Vandenburg Air Force Base to act as primary communications lines associated with Peace Keeper (MX) ICBM (intercontinental ballistic missile) flight tests as well as surface test command, control, and monitoring. These are typical U.S. military fiber optic equipment applications at the present time [3].

At the same time, the Air Force also plans to take fiber optics and use them in specially dispatched interceptors (SDI) and advanced tactical fighters (ATF), facilitating the avoidance of discovery and attack associated with enemy radars [3].

III. OPTICAL FIBER TECHNOLOGY USED IN GUIDED MISSILES

On the basis of introductions by the U.S. Corning Glass company, the U.S. Army and Navy are just in the midst of carrying out R&D projects in order to develop a new type model of wire guided missile, designated FOG-M (fiber optic guided missile). Fig.3 is a fiber optic guided missile schematic and control line and block chart [3,4]. Missiles are equiped with image sensors.

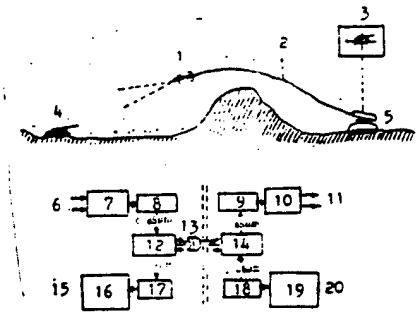

Fig.3 Fiber Optic Controled Missile Schematic and Control Line and Block Chart 1. Missile 2. Optical Cable 3. Image Display 4. Target 5. Missile Vehicle 6. Video Frequency Input TM Signal 7. Signal Regulation and Encryption 8 and 18. Laser Diode Transmiter 9 and 17. Receiver 10. Signal Processor 11. Video Frequency Output TM Signal 12 and 14. Two Way Coupler 13. Fiber Optic Tube 15 and 20. Command Signals 16. Signal Separation 17. Multichannel Modulation

Missiles are launched from behind mountains. Through fiber optics, imagery taken by the missile of targets and background are sent to the launch point, and gunners use this to indentify and select targets, sending out control commands to missiles. This is one type of missile tracking method. Experimental systems associated with this type of method were intially set up by the U.S. Hughes company and International Telegraph and Telephone company. Electronic equipment was supplied by the International Telegraph and Telephone company photoelectric products department, fitted with 1.06μm light emiting diodes associated with up links and 0.85μm or 1.3μm lasers used in down links. Systems make use of two wave division compound use communications channels, utilizing optical fibers to carry out transmissions in opposite directions [4(illegible)]. The reason is that high level imagery signal processing and guidance calculations are carried out at launch points. Therefore, it is possible to carry out high precision guidance, and it is not easy to be detected and jammed by the enemy. Firing points are concealed and they are able to identify friend or foe in defense of close combat, selecting targets. /49

Antitank weapon systems in the Fig. have already gone through 12 iterations of successful firings in the U.S. state of

Alabama. During the experiments, missiles were fired vertically to approximately 200m altitudes. In conjunction with this, pitched flights were several thousand meters. Gunners guide missiles by signals received from warhead television cameras. In the final flight phase of missiles, missiles automatically track and directly hit targets. This project was the U.S. development project with the greateast and most practical use during the five year period 1986-1990, with an investment of 645 million U.S. dollars [3]. This type of FOG-M is most appropriate for use in vehicle launches. If launched from bases, it is possible to lower launch vehicle costs. According to briefings--opting for the use of this type of project--it is possible at the present time to guide 18 thousand missiles. Each missile has a price of approximately 22 thousand U.S. dollars. In conjunction with this, plans opt for the use of 8.3μm single mode optical fiber with a wrapping layer outside diameter of 125μm [3].

The U.S. Air Force also takes fiber optic technology and uses it in launched cruise missiles (GLCM). In conjunction with this, option is made for the use of AN/GRC-206 tactical radios to control aircraft. At the time of each launch iteration, in all cases, they are equiped with two controlable trailers and four sets of launching racks. The entire system is, in all cases, interconnected with complicated optical cables [3]. Launching racks are connected to trailers by two sets of six circuit optical fiber, receiving test measurement and ignition commands. GRC-206 radio systems opt for the use of two way optical cable in order to facilitate connections to television systems, providing forward edge command post combat zone monitoring. This type of optical cable system designed by the U.S. Westinghouse company has already been delivered to Australian and Egyptian air force air defense radar system detachments for use.

IV. OPTICAL FIBER TECHNOLOGY USED IN GUIDED TORPEDOES, LAUNCHED REMOTE CONTROL AIRCRAFT, AND MINE LAYING

The U.S. Navy is in the midst of carrying out research associated with fiber optically guided torpedoes. Fig.4 is a schematic diagram for U.S. fiber optically guided torpedoes [2(illegible]. This system is figured for use in order to guide in torpedoes launched from sumbarines or other launching platforms. Torpedo guidance ranges are capable of reaching 100km or more, exceeding weapon ranges. The systems in question possess their own passive sonar electric power in order to drive fiber optically guided torpedoes. Not only are they not easy for the enemy to detect. Moreover, specially dispatched long range detachment launching platforms are also capable of firing this type of torpedo. When torpedoes approach targets, selection is

made of important targets to carry out attacks.

Through fiber optic remote control command detonation to the surface, it is easy to form minefields. Mines are equiped with imargery sensors and television cameras. They are not only capable of identifying friend or foe. They are, moreover, capable of indicating before hand high targets and low targets. Before friendly forces have gone on the offensive, it is possible to first lay mines. After that, friendly forces go on the offensive in the minefields. As far as enemy harbors, warship anchorages, or sea lanes are concerned, it is possible to do monitoring and control with fiber optic information networks. As far as sea beaches connected to the land are concerned, operating personnel are capable of using laser optics to lay mines outside of harbors [3].

According to Hughes company reports, fiber optics are used in the launch of remote control drones during aircraft flights. This type of drone flies in front of aircraft. It first supplies early warning information and determinations of target direction.

If the vicinity of the target is too dangerous, it is possible to first guide drones toward targets. In conjunction with this, flights are under ground command. They are like complicated model airplanes. The small model aviation guidance equipment on them is capable of recovery to the surface. [293(illegible)]

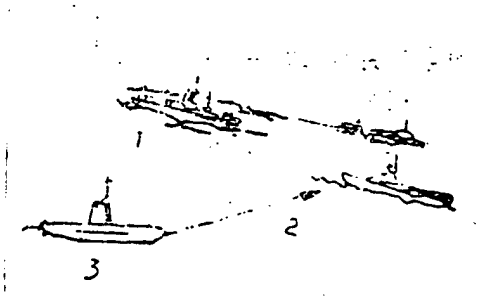

Fig.4 Schematic Diagram of Fiber Optic Guided Torpedoes the U.S. Navy Opted for the Use of. 1. Launching Vessel Stops Outside of Enemy Defended Areas in Order to Increase Survivability. 2. In Order to Hit Targets, Outputed Signals Associated with Passive Detectors Return to Launching Vessel. 3. Contact Is Picked Up with the Launching Vessel and Communications Line Media Are Not Easily Detected.

V. FIBER OPTIC SENSORS

/50

Fiber optic sensors are a type of new model fiber optic component. Consideration was already given to them early on during research on fiber optic information transmission. They take measured objects and pick them up acting as optical signals.

They are superior to electrical sensors and are capable of measuring objects which are difficult to measure, such as, high voltage, electromagnetic, underwater, optical radiations associated with nuclear reactions, as well as chemical atmospheres, and so on. Moreover, transmission losses are low. It is not necessary to consider relationships between the relative positions of measurement instruments and measured objects.

U.S. development of fiber optic sensors was first given to the naval research laboratories (NRL). Initial investment was primarily from the Defense Advanced Research Project Agency. In the research, probes were done of the possiblity of their use in various areas outside underwater sonic sensing--for example, rotation sensors, magnetic field sensors, aviation sonic sensors, pressure sensors, and so on [5].

In the years 1986-1990, the most use was in sonic sensors and spin sensors (fiber optic gyroscopes). In these, sonic sensors are used in antisubmarine warfare observation. Rotating sensors are capable of improving the inertial guidance systems of tactical missiles and aircraft in order to strengthen ground or air launched cruise missiles and F-16C/D [3].

On this basis, McDonell Douglas aerospace company is just in the midst of developing a type of fiber optic laser gyroscope which deviates one degree each hour and has digital output. This type of optical fiber gyroscope will compete with small model ring shaped laser gyroscopes [294].

According to the U.S. Corning Glass company briefings, opting for the use of interference measurement techniques associated with sonic sensors to use in data processing has great potential. The company in question is just in the midst of considering "full optic" torpedoes. This type of torpedo not only opts for the use of fiber optics associated with sonic sensors and guidance lines. Moreover, data processing circuit systems and launch control systems also use composite optical systems as replacements [3].

At the present time, the U.S. Air Force has already opted for the use of new model micorwave/millimeter wave integrated circuits (MIMIC) and forward end sensors constructed of GaAs components in order to equip a new generation of aircraft. As far as this type of sensor fitted on the forward end of aircraft

is concerned--with regard to processing information associated with transmiting and receiving modules--signals are made not to return again to instrument modules for processing. Among these, scanning rates associated with electronic control phase shift devices use millisecond level measurements on B-1 bombers at the present time. If option is made for the use of fiber optics capable of going down to millisecond level measurements, multiple beam and phase system capacities will very, very greatly improve [3].

VI. CONCLUSION

This article introduces applications of fiber optic technology in U.S. military fields. Among these, the most numerous applications are military fiber optic communications, fiber optic guided missiles, and fiber optic sensors. Seen from the point of view of tactics, fiber optic technologies will play important roles in future wars. Whoever first masters fiber optic technology, and, in conjunction with that, uses it to equip units, will then hold the initiative on the battlefield. This is nothing else than the reason for U.S. investments in military fiber optic technologies doubling and redoubling year by year. Following along with improvements in fiber optic technologies and the development of industrial processes associated with fiber optics, the range of applications will also expand without ceasing.

REFERENCES

〔1〕 《国外激光》, 1983年, 第11期, 第2页。

〔2〕 《战略防御》, 1987年, 第5期, 第34页。

〔3〕 Laser Focus, 1987, Vol. 23, No. 8, P. 94～106.

〔4〕 International defense review, 1984, No. 2, P. 151～154.